



## NRC Publications Archive Archives des publications du CNRC

### **Performance evaluation of different configurations of biogas-fuelled SOFC micro-CHP systems for residential applications**

Farhad, Siamak; Hamdullahpur, Feridun; Yoo, Yeong

This publication could be one of several versions: author's original, accepted manuscript or the publisher's version. / La version de cette publication peut être l'une des suivantes : la version prépublication de l'auteur, la version acceptée du manuscrit ou la version de l'éditeur.

For the publisher's version, please access the DOI link below. / Pour consulter la version de l'éditeur, utilisez le lien DOI ci-dessous.

#### **Publisher's version / Version de l'éditeur:**

<https://doi.org/10.1016/j.ijhydene.2010.01.052>

*International Journal of Hydrogen Energy*, 35, 8, pp. 3758-3768, 2010-04-01

#### **NRC Publications Record / Notice d'Archives des publications de CNRC:**

<https://nrc-publications.canada.ca/eng/view/object/?id=7fbe2fe7-5ead-4903-944e-9541e107aa82>

<https://publications-cnrc.canada.ca/fra/voir/objet/?id=7fbe2fe7-5ead-4903-944e-9541e107aa82>

Access and use of this website and the material on it are subject to the Terms and Conditions set forth at

<https://nrc-publications.canada.ca/eng/copyright>

READ THESE TERMS AND CONDITIONS CAREFULLY BEFORE USING THIS WEBSITE.

L'accès à ce site Web et l'utilisation de son contenu sont assujettis aux conditions présentées dans le site

<https://publications-cnrc.canada.ca/fra/droits>

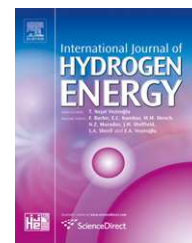
LISEZ CES CONDITIONS ATTENTIVEMENT AVANT D'UTILISER CE SITE WEB.

**Questions?** Contact the NRC Publications Archive team at

PublicationsArchive-ArchivesPublications@nrc-cnrc.gc.ca. If you wish to email the authors directly, please see the first page of the publication for their contact information.

**Vous avez des questions?** Nous pouvons vous aider. Pour communiquer directement avec un auteur, consultez la première page de la revue dans laquelle son article a été publié afin de trouver ses coordonnées. Si vous n'arrivez pas à les repérer, communiquez avec nous à PublicationsArchive-ArchivesPublications@nrc-cnrc.gc.ca.



Available at [www.sciencedirect.com](http://www.sciencedirect.com)journal homepage: [www.elsevier.com/locate/he](http://www.elsevier.com/locate/he)

# Performance evaluation of different configurations of biogas-fuelled SOFC micro-CHP systems for residential applications

Siamak Farhad<sup>a</sup>, Feridun Hamdullahpur<sup>b,\*</sup>, Yeong Yoo<sup>c</sup>

<sup>a</sup> Department of Mechanical and Aerospace Engineering, Carleton University, 1125 Colonel By Dr. Ottawa, ON K1S 5B6, Canada

<sup>b</sup> Department of Mechanical and Mechatronics Engineering, University of Waterloo, 200 University Avenue, West Waterloo, ON N2L 3G1, Canada

<sup>c</sup> Institute for Chemical Process and Environmental Technology, National Research Council of Canada, 1200 Montreal Road. Ottawa, ON K1A 0R6, Canada

## ARTICLE INFO

### Article history:

Received 28 October 2009

Received in revised form

24 December 2009

Accepted 15 January 2010

Available online 9 February 2010

### Keywords:

Solid oxide fuel cell

Micro-combined heat and power system

Biogas

Residential application

Anode gas recirculation

Steam reforming

Partial oxidation

## ABSTRACT

Three configurations of solid oxide fuel cell (SOFC) micro-combined heat and power (micro-CHP) systems are studied with a particular emphasis on the application for single-family detached dwellings. Biogas is considered to be the primary fuel for the systems studied. In each system, a different method is used for processing the biogas fuel to prevent carbon deposition over the anode of the cells used in the SOFC stack. The anode exit gas recirculation, steam reforming, and partial oxidation are the methods employed in systems I–III, respectively. The results predicted through computer simulation of these systems confirm that the net AC electrical efficiency of around 42.4%, 41.7% and 33.9% are attainable for systems I–III, respectively. Depending on the size, location and building type and design, all the systems studied are suitable to provide the domestic hot water and electric power demands for residential dwellings. The effect of the cell operating voltage at different fuel utilization ratios on the number of cells required for the SOFC stack to generate around 1 kW net AC electric power, the thermal-to-electric ratio (TER), the net AC electrical and CHP efficiencies, the biogas fuel consumption, and the excess air required for controlling the SOFC stack temperature is also studied through a detailed sensitivity analysis. The results point out that the cell design voltage is higher than the cell voltage at which the minimum number of cells is obtained for the SOFC stack.

© 2010 Professor T. Nejat Veziroglu. Published by Elsevier Ltd. All rights reserved.

## 1. Introduction

Biogas is a renewable and alternative source of fuel that can assist to reduce the consumption of fossil fuel and emission of greenhouse gases. This gas, which is mostly produced using anaerobic digestion or fermentation of biodegradable materials such as biomass, manure, sewage, and municipal waste,

has been recognized by the United Nations development program as one of the important decentralized sources of energy [1].

Biogas, which contains mainly methane and carbon dioxide, can be used as a fuel in a solid oxide fuel cell (SOFC) to generate electric power with high efficiency and low environmental impact [2–7]. An SOFC can achieve satisfactory

\* Corresponding author. Tel.: +1 519 888 4766; fax: +1 519 885 5862.

E-mail addresses: [siamak\\_farhad@yahoo.com](mailto:siamak_farhad@yahoo.com) (S. Farhad), [fhamdull@uwaterloo.ca](mailto:fhamdull@uwaterloo.ca) (F. Hamdullahpur).

0360-3199/\$ – see front matter © 2010 Professor T. Nejat Veziroglu. Published by Elsevier Ltd. All rights reserved.

doi:10.1016/j.ijhydene.2010.01.052

**Nomenclature**

$C_p$	heat capacity at constant pressure ( $\text{kJ kg}^{-1} \text{K}^{-1}$ )
$ex$	specific exergy ( $\text{kJ kg}^{-1}$ )
$\dot{E}x$	exergy (W)
$h$	specific enthalpy ( $\text{kJ kg}^{-1}$ )
$k$	heat capacity ratio (–)
LHV	lower heating value ( $\text{kJ kg}^{-1}$ )
$\dot{m}$	mass flow rate ( $\text{kg s}^{-1}$ )
$p$	pressure (Pa)
$T$	temperature (K)
$U_f$	fuel utilization ratio (%)
$\dot{W}$	electric power (W)

*Greek letters*

$\eta$	efficiency (–)
--------	----------------

performance even if the methane content of the biogas is not high. Laboratory tests, performed by Jenne et al. (2002), confirmed that the efficiency of the SOFC drops by approximately 5% when the mole fraction of methane in the fuel decreases from 70% to 30% [8]. Yi et al. (2005) showed that the electrical efficiency of an integrated SOFC system drops around 1.1% if biogas is used instead of natural gas [9].

Biogas can be directly fed and internally reformed in an SOFC stack; however, carbon deposition may occur and gradually deactivate the SOFC anode catalysts [10–15]. Another problem of internal reformation of biogas is a large temperature gradient in the SOFC stack due to a significant cooling effect caused by the fast internal steam reforming reaction [16]. To relieve these problems, biogas can be processed in an appropriate fuel processor before using in the SOFC stack [17]. The steam reforming [18–20], partial oxidation [21,22], and auto-thermal reforming [23,24] are typical fuel processing methods which are usually suggested for SOFC systems. In addition to these fuel processing methods, anode exit gas recirculation [25,26] can be applied to prevent carbon deposition over the anode catalyst.

Several researchers have suggested the application of SOFC systems to generate electric power and thermal energy required for residential dwellings [27–32]. For this application of SOFC systems, the thermal energy to electric power ratio (TER) generated in the SOFC system and the TER required for residential dwellings should match. The TER for residential dwellings can be determined based on space heating, space cooling, or domestic hot water demands and its magnitude is highly dependent on location, building type, design, usage pattern, time of day, and time of year [33]. The TER for hourly averaged annual domestic hot water for a 200 m<sup>2</sup> house can range from 0.7 to 1.0 [34]. The TER for space heating can be substantially higher (more than ten times) than that for domestic hot water in cold climates [33].

In this paper, three biogas-fuelled SOFC micro-combined heat and power (micro-CHP) systems for application in residential dwellings are evaluated through computer simulation. In each system, a different method is used for processing the biogas fuel to prevent carbon deposition over the anode of the cells used in the SOFC stack. The anode exit gas recirculation,

steam reforming, and partial oxidation are the methods employed in these systems.

## 2. Systems description

The configuration of the systems studied in this paper is shown in Fig. 1. These systems are mainly composed of an SOFC stack used to generate DC electric power and heat; an air heater used to increase the temperature of the air before it enters the SOFC stack; an air blower used to overcome the pressure drop in the system; a burner used to convert the chemical energy of the unutilized fuel in the SOFC stack to heat; a boiler used to generate hot water for a residential dwelling; an inverter used to invert the DC electric power to AC; and a reformer control volume that contains a biogas clean-up system, heater(s) and/or reformer.

As shown in Fig. 1, three streams of biogas, air, and cold water enter the systems. The composition of the biogas used in this study is the averaged composition of the biogas produced in wastewater treatment plants in Ontario. This gas contains methane (60.8%), carbon dioxide (34.8%), nitrogen (2.4%), oxygen (1.5%), and water vapor (0.01%). The range of hydrogen sulfide and silicon compounds in this gas is 2.5–3450 and 0–2500 ppm, respectively. The other compounds such as toluene, benzene, methyl chloride, and chlorofluorocarbons are present at levels below 10 ppm [35]. The composition of this gas is shown in the C–H–O ternary diagram in Fig. 2. As shown in this figure, the biogas is located above the carbon deposition boundary (CDB) curves, indicating that carbon deposition over the anode catalyst in SOFCs is possible. As explained in [36,37], the location of the biogas can be moved to below the CDB curves by adding sufficient anode exit gas, water, or air to the biogas fuel in the reformer control volume. Of course, it is possible to move the location of the biogas to below the CDB curves by adding CO<sub>2</sub>, but providing a suitable source of CO<sub>2</sub> for the operation of the SOFC system in residential dwellings is complicated. Hence, we do not consider the effect of adding CO<sub>2</sub> and dry reforming of the biogas in this study.

In all systems studied, the biogas enters a gas clean-up system where the contaminants in the biogas are reduced to levels that will not damage the anode and/or reformer catalysts. Depending on the operating temperature of the gas clean-up system, a heat exchanger may be required before cleaning the biogas. The most attractive and convenient method to remove hydrogen sulfide from the biogas in gas clean-up systems is the use of an activated carbon bed. This method is highly effective at relatively low loadings of hydrogen sulfide ( $\text{H}_2\text{S} < 200$  ppm) [38]. In the case of high hydrogen sulfide content, additional removal technologies are required to reduce the hydrogen sulfide content to below 200 ppm. A similar absorption bed can be used to remove silicon compounds that may cause a significant deactivation of the anode catalyst [35]. After cleaning the biogas, it should be processed before entering the SOFC stack. Therefore, in system I, after passing the cleaned biogas through a heat exchanger in the reforming control volume and increasing its temperature, the high temperature cleaned biogas is mixed with the anode exit gas (line 15 (I) in Fig. 1). In system



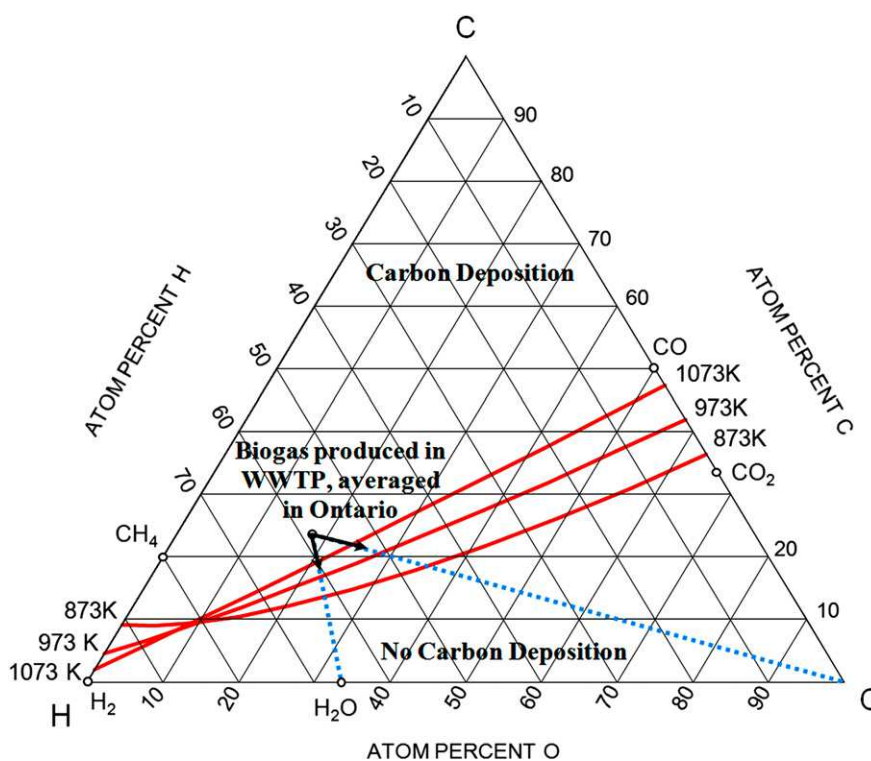


**Fig. 2 – The location of the averaged composition of the biogas produced in wastewater treatment plant in Ontario and CDB curves at atmospheric pressure and temperatures of 873 K, 973 K, and 1073 K in the C–H–O ternary diagram.**

including the electrochemical reactions (R1) and (R4) in the anode and cathode, respectively, and the steam reforming and water gas shift reactions (R2) and (R3) in the anode were considered in the computer code and the activation, ohmic, and concentration polarizations were determined. The detail description of the modeling of polarizations used in the computer code is presented in Refs. [39–42]. It should be noted that the inlet and outlet fuel streams from the anode were assumed to be in thermodynamic equilibrium in the cell modeling.

The SOFC stack was modelled by extending the cell model. Since heat transfer from the SOFC stack affects cell performance, an insulation system is required to control this heat transfer. The insulation system considered in this study consists of an insulation layer mechanically supported by two metal layers. To determine the rate of heat transfer from the SOFC stack, the conductive heat transfer in the insulation layer and the radiative and natural convective heat transfer from the outer metal layer were taken into account. The effect of the heat transfer from the SOFC stack on the cell's performance was considered in the computer code. The power output obtained from an SOFC stack is usually less than that obtained from a single cell multiplied by the number of cells used in the SOFC stack due to the gas and electron leakages and the effect of bipolar plates in the stack. To reflect these effects on the power output from the SOFC stack in the computer simulation, we assumed a 5% voltage drop in Current-Voltage (CV) characteristics of the SOFC stack in comparison with single cells.

The balance of plant (BoP) components such as the air heater, blower, boiler, reformer, and burner were thermodynamically modelled under steady state operating conditions. The properties, composition and flow rate of all streams in the three systems were determined after modeling the BoP components. Then, the net AC electric power, heat produced, electrical efficiency, CHP efficiency, and total exergy destruction of the systems were determined from Eqs. (1) to (5), respectively. It should be noted that the effects of the boiler feedwater pump, the biogas blower, and the heat transfer from the BoP components on the electrical and CHP efficiencies and exergy destruction of the systems were not taken into account in this study.

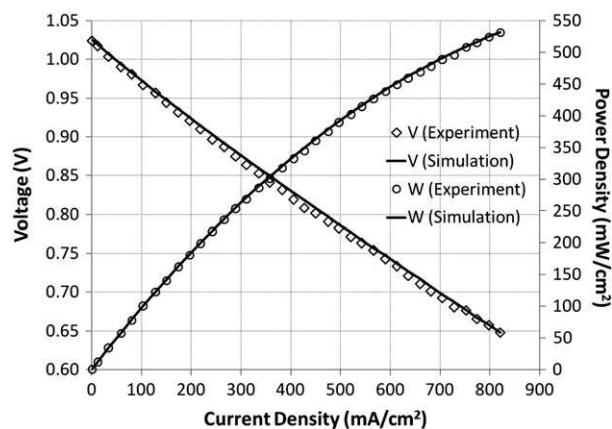


**Fig. 3 – Results of the computer simulation and experiment for a commercially available electrolyte supported cell (ESC 4).**

**Table 1 – Input data for computer simulation of the biogas-fuelled SOFC micro-CHP systems for residential applications.**

Parameter	Value
Cell operating temperature	850 °C
Cell operating pressure	1 atm
Fuel inlet temperature to the SOFC stack	750 °C
Air inlet temperature to the SOFC stack	700 °C
Fuel utilization ratio	60%, 70%, 80%
Anode and cathode	
Thickness	40 μm
Porosity (assumed)	0.33 (-)
Tortuosity (assumed)	4 (-)
Electrolyte thickness	90 μm
Interconnect thickness	3000 μm
Cell active length	10 cm
Cell active width	10 cm
Insulation system of the SOFC stack	
Thickness	50 mm
Thermal conductivity	0.025 Wm <sup>-1</sup> K <sup>-1</sup>
Emissivity of the outer surface of the SOFC stack	0.8 (-)
Number of cells in the SOFC stack	27
Net AC electric power output from the SOFC system	≈ 1 kWe
Pressure drop in the system	0.3 bar
Air blower efficiency	62.5%
Inlet cold water temperature to the boiler	40 °C
Outlet hot water temperature from the boiler	90 °C
Efficiency of DC to AC inverter	92%
Flue gas exhaust temperature	T <sub>dewPoint</sub> + 50 °C
Pinch temperature of the boiler	>20 °C

$$\dot{W}_{\text{net AC electric}} = \dot{W}_{\text{SOFC stack}} \times \eta_{\text{inverter}} - \dot{W}_{\text{blower}} \quad (1)$$

$$\dot{Q} = \dot{m}_{\text{cold water}}(h_{\text{hot water}} - h_{\text{cold water}}) \quad (2)$$

$$\eta_{\text{electric}} = \frac{\dot{W}_{\text{net AC electric}}}{\dot{m}_{\text{biogas}} \text{LHV}_{\text{biogas}}} \quad (3)$$

$$\eta_{\text{CHP}} = \frac{\dot{W}_{\text{net AC electric}} + \dot{Q}}{\dot{m}_{\text{biogas}} \text{LHV}_{\text{biogas}}} \quad (4)$$

$$\dot{E}x_{\text{destruction, total}} = \dot{m}_{\text{biogas}} ex_{\text{biogas}} - \dot{W}_{\text{net AC electric}} - (\dot{E}x_{\text{hot water}} - \dot{E}x_{\text{cold water}}) \quad (5)$$

In Eq. (1), the blower input power is determined from the following equation [50]:

$$\dot{W}_{\text{blower}} = \dot{m}_{\text{air}} C_{p,\text{air}} T_5 \left( \left( \frac{p_6}{p_5} \right)^{\frac{k_{\text{air}}-1}{k_{\text{air}}}} - 1 \right) \frac{1}{\eta_{\text{blower}}} \quad (6)$$

After determining the net electric power and the heat produced in the system, the TER of the system can be obtained from Eq. (7).

$$\text{TER} = \frac{\dot{Q}}{\dot{W}_{\text{net AC electric}}} \quad (7)$$

To prevent carbon deposition over the anode catalyst, the minimum required flow rate of the anode exit gas recirculation for system I, water for system II, and air for system III was determined after obtaining the carbon deposition boundary. The carbon deposition boundary is determined using the three reactions of carbon decomposition (R5) [43], CO reduction (R6), and the Boudouard reaction (R7) [36].



#### 4. Validation of the computer code

To validate the computer code at the cell level, the performance of a commercially available electrolyte supported cell (ESC 4) produced by H.C. Starck Company [44] was simulated. This cell is composed of Ni/GDC (Gadolinia-doped Ceria) anode, dense YSZ electrolyte and YSZ/LSM (lanthanum strontium manganese oxide) cathode. The Ni/GDC anode of this cell is more resistant against carbon deposition than the Ni/YSZ anode [45]. To simulate this cell, it was assumed that the porosity and tortuosity of

**Table 2 – The results obtained from the computer simulation for the SOFC micro-CHP systems at fuel utilization ratios of 80%, 70%, and 60%.**

Fuel utilization ratio (%)	System I			System II			System III		
	80	70	60	80	70	60	80	70	60
Reforming agent to biogas ratio (kg kg <sup>-1</sup> )	0.63	0.68	0.74	0.29	0.29	0.29	1.08	1.08	1.08
Biogas mass flow rate (kg h <sup>-1</sup> )	0.432	0.443	0.475	0.436	0.454	0.508	0.536	0.59	0.662
AC electrical efficiency (%)	42.4	40.5	37.5	41.7	38.7	34.5	33.9	30.7	27.4
CHP efficiency (%)	76.9	78.4	80.4	72.9	75.1	77.6	80.5	82.5	84.5
TER (-)	0.81	0.94	1.15	0.75	0.94	1.25	1.38	1.68	2.09
Excess air (-)	5.2	4.2	3.3	4.9	3.9	3.1	5.1	4.2	3.4
Operating voltage of system (V)	16.3	16.9	17.3	16.5	17.1	17.5	16.3	16.7	17.1
Total exergy destruction of system (W)	1338	1401	1568	1369	1491	1751	1858	2122	2473
Blower input power (W)	156	132	119	141	118	105	158	145	132
Generated hot water (kg h <sup>-1</sup> )	13.5	15.2	18.5	12.2	15.0	19.8	22.6	27.6	34.3
Exit flue gas temperature (°C)	79.1	82.1	85.0	85.5	88.9	92.5	82.4	85.2	88.6

**Table 3 – Reference species of the atmospheric air [46].**

Compound	%mol
Ar	0.912
CO <sub>2</sub>	0.0337
D <sub>2</sub> O	0.000344
H <sub>2</sub> O	2.215
He	0.000488
Kr	0.000098
N <sub>2</sub>	76.305
Ne	0.00178
O <sub>2</sub>	20.531
Xe	0.000088

electrodes are 0.33 and 4, respectively. The voltage and power density of the ESC 4 cell obtained by the computer simulation and the experiment at various current densities and the cell operating temperature of 850 °C are shown in Fig. 3. The computer code could predict the voltage and power density of the ESC 4 cell with an average relative error of ±1%.

## 5. Input data

The input data used for evaluation of the systems studied for residential applications are listed in Table 1. The SOFC stack used in these systems consists of twenty-seven ESC 4 cells that operate at the temperature, pressure and voltage of around 850 °C, 1 atm, and 0.7 V, respectively. Each system generates around 1 kW net AC electric power after deducting the power required for the internal consumption of the system. It is also considered that the exhaust gases leave the systems at a temperature which is 50 °C greater than the dew point temperature of the exhaust gases. It should be noted that the dew point temperature is calculated based on the partial pressure of the water vapour in the exhaust gases.

## 6. Results and discussions

Based on the input data presented in Table 1, the results of the computer simulation for all three systems studied are obtained and listed in Table 2.

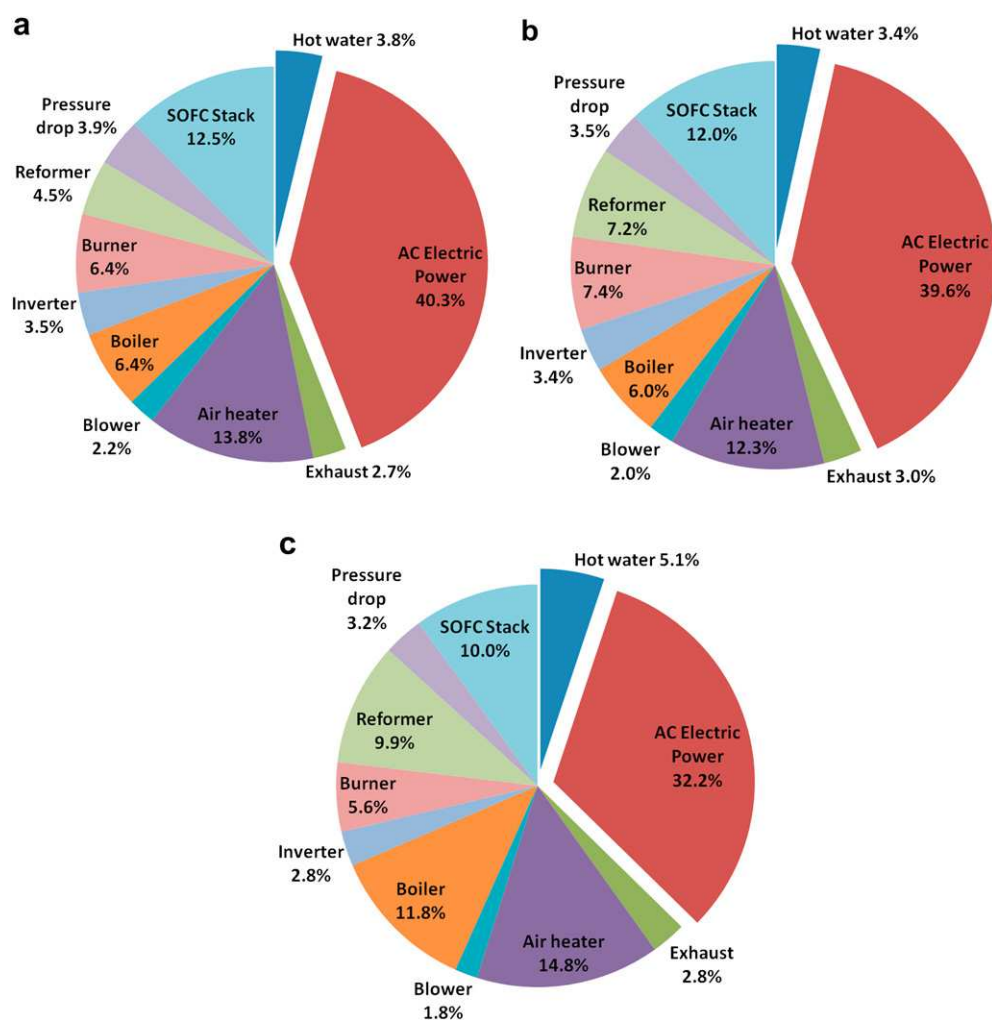


**Fig. 4 – The share of each component in the exergy destruction of the input biogas to (a) system I with anode exit gas recirculation, (b) system II with steam reforming, and (c) system III with partial oxidation fuel processor, at the fuel utilization ratio of 80%.**

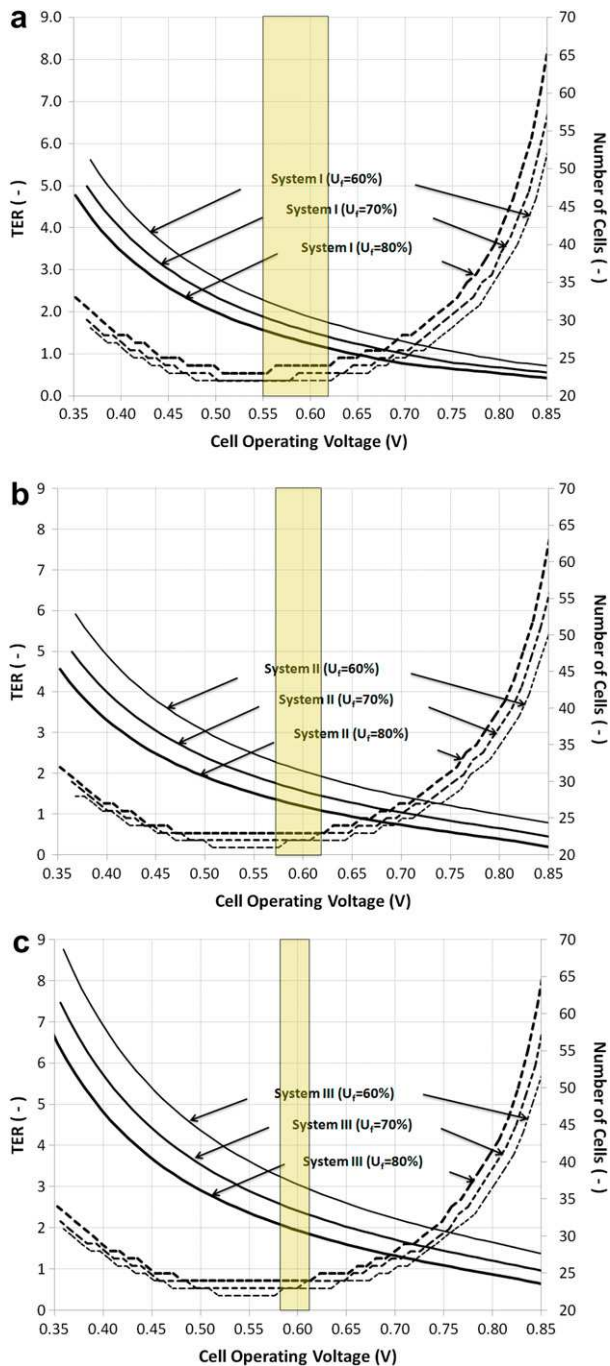


**Fig. 5** – Effect of the cell operating voltage at fuel utilization ratios of 80%, 70%, and 60%, on the number of cells in the SOFC stack (dashed lines) and TER (solid lines) in (a) system I with anode exit gas recirculation, (b) system II with steam reforming, and (c) system III with partial oxidation fuel processor (the yellow column indicates the range of cell voltages at which the minimum number of cells is required in the SOFC stack operated with fuel utilization ratios between 60% and 80%).

The minimum mass flow rate of the reforming agent required for each system, to prevent carbon deposition over the anode catalyst of the ESC 4 cell, is determined using the computer simulation. As shown in Table 2, the minimum mass

flow rate of the anode exit gas for system I depends on the fuel utilization ratio, and it is equal to 0.63, 0.68, and 0.74 of the input biogas mass flow rate at the fuel utilization ratios of 80%, 70% and 60%, respectively. The minimum mass flow rate of the input water to the reforming control volume of system II, and the input air to the reforming control volume of system III is 0.29 and 1.08 of the input biogas mass flow rate, respectively, and these values are independent of the fuel utilization ratio.

According to the computer simulation results, at the fuel utilization ratio of 80%, the inlet biogas flow rate to systems I to III is approximately 0.432 kg/h, 0.436 kg/h and 0.536 kg/h, respectively. This result shows that the inlet biogas mass flow rate to system I is the lowest among the systems studied. System I also exhibits a net AC electrical efficiency of 42.4% at the fuel utilization ratio of 80%, followed by system II with 41.7%, and system III with 33.9%. System III provides the highest CHP efficiency among the systems studied, followed by systems I and II. The CHP efficiency of systems I to III is around 76.9%, 72.9%, and 80.5%, respectively, at the fuel utilization ratio of 80%. The TER of systems I and II at the fuel utilization ratio of 70% and 80% is well-matched with the TER based on the domestic hot water demands for single-family detached dwellings [34]. The studies show that the TER of system III is suitable for this application at the fuel utilization ratio of 90%. The excess air required for controlling the temperature of the SOFC stack is the lowest for system II, and so the size and initial investment cost of the blower, air heater, and burner is the lowest for this system among the systems studied. The operating voltage of system II is the highest among the studied system. At the fuel utilization ratio of 80%, the voltage level reaches around 16.5 V for system II and 16.3 V for systems I and III. The total exergy destructions in systems I and II are very close, especially at fuel utilization ratios greater than 80%, and are substantially less than that in system III. The studies also indicate that depending on the fuel utilization ratio and the system configuration, 10% to 16% of the electric power generated in the SOFC stack is consumed in the air blower.

### 6.1. Exergy analysis

Excluding nuclear, magnetic, electrical, and interfacial effects, the exergy of a stream can be divided into four components of physical, chemical, kinetic, and potential exergies. In this study, it is assumed that the changes of the inlet and outlet kinetic and potential exergies of a stream are negligible in comparison with the physical and chemical exergies. To calculate the physical and chemical exergies, the reference atmospheric air species listed in Table 3, and the reference temperature, pressure, and relative humidity of 298.15 K, 101325 Pa, and 70%, respectively, are taken into account. After finding the exergy of the streams, the exergy destruction of a component is obtained from the difference between the exergy of the input and output streams from the component with the consideration of the exergy of the heat and work to or from the component.

To determine the share of each component of the systems studied in the exergy destruction of the input biogas, an extensive exergy analysis at the cell fuel utilization ratio of 80% was performed and the results are illustrated in Fig. 4. As

**Table 4 – The cell operating voltage at which the minimum number of cells is obtained for the systems studied, at fuel utilization ratios of 60%, 70%, and 80%.**

Fuel utilization ratio (%)	System I			System II			System III		
	60	70	80	60	70	80	60	70	80
Cell operating voltage (V)	0.62	0.58	0.55	0.57	0.61	0.62	0.58	0.60	0.61
Minimum number of cells (-)	21	22	23	21	22	23	22	23	24

shown in this figure, the exergy destruction in the SOFC stack is not as significant as in the air heater, because the heat generated due to polarizations in the high temperature ESC 4 cells can still generate additional electricity in other power generation devices. The air heater has the largest share in the exergy destruction of the input biogas in all the studied systems, followed by the SOFC stack and burner/boiler for system I, the SOFC stack and burner/boiler for system II, and the boiler and SOFC stack for system III. There is the potential to generate additional electric power in these systems, especially in system III, if they are combined with other power generation devices and appropriately optimized using pinch technology and exergy analysis [47,48].

## 6.2. Sensitivity analysis

The results listed in Table 2 were obtained for the SOFC stack with twenty-seven ESC 4 cells. Since the SOFC stack represents 30–50% of the initial investment cost of an SOFC system [49], the number of cells has an important role to economically optimize the SOFC system. Two key parameters that affect the number of cells in the SOFC stack are the cell operating voltage, which is the average of the single cell voltages, and the fuel utilization ratio [50]. In this study, a correlation between the cell operating voltage at different fuel utilization ratios and the number of cells required for the SOFC stack to generate around 1 kW net AC electric power for residential dwellings is established through a detailed sensitivity analysis. Since the cell operating voltage and fuel utilization ratio affect the TER, excess air, and electrical and CHP efficiencies, these parameters are also monitored during the sensitivity analysis. It should be noted that our study does not cover the influence of the cell operating voltage and fuel utilization ratio on the durability and thermo-mechanical reliability of the cell.

### 6.2.1. Effect of the cell operating voltage and fuel utilization ratio on the number of cells and TER

As shown in Fig. 5, the number of cells required for the SOFC stack to generate around 1 kW net AC electric power for residential dwellings changes approximately as a concave upward parabolic curve with the cell operating voltage for all the systems studied. Indeed, the number of cells first reduces with decreasing the cell operating voltage and then increases. The cell operating voltage at which the minimum number of cells required in the SOFC stack is obtained is called “mCV” in this study, which is a function of the fuel utilization ratio.

The mCV for each system at fuel utilization ratios of 60%, 70%, and 80% has been determined and listed in Table 4. As

shown in this table, for fuel utilization ratios between 60% and 80%, the range of mCVs is obtained between 0.55 V and 0.62 V for system I, 0.57 V and 0.62 V for system II, and 0.58 V and 0.61 V for system III. These voltage ranges are shown with yellow columns in Figs. 5 and 6.

Based on the mCV, The operating voltages of a cell can be divided into two groups; those which are less than mCV (Group I) and those larger (Group II). Considering this classification, we will show that the optimum operating voltage of a cell always falls in Group II of the cell category.

As shown in Fig. 5, with decreasing the cell voltage, the number of cells required for the SOFC stack increases for Group I and decreases for Group II of the cell voltages. For both groups of voltages, the number of cells also decreases with decreasing the fuel utilization ratio.

As shown in Fig. 5, the TER of all the systems studied increases progressively with decreasing the cell operating voltage. The TER also increases with decreasing the fuel utilization ratio, because the fuel unutilized in the SOFC stack can be used in the burner to generate additional heat for the boiler to produce more hot water for residential dwellings. For Group I of the cell voltages, the TER of all the systems studied is greater than unity. It means, the heat produced in these systems is more than the heat required for the domestic hot water demand for single-family detached dwellings.

### 6.2.2. Effect of the cell operating voltage and fuel utilization ratio on electrical and CHP efficiencies

Fig. 6 illustrates the effect of the cell operating voltage at different fuel utilization ratios of 60%, 70%, and 80%, on the electrical and CHP efficiencies of the systems. As shown in this figure, an increase in the operating voltage of the cell leads to a linear increase in the net AC electrical efficiency of all the systems studied. In the range of the fuel utilization ratios investigated, the net AC electrical efficiency is higher at elevated fuel utilization ratios.

The CHP efficiency of all the systems studied decreases linearly with a slight slope with increasing the cell operating voltage to around 0.7 V. If the cell operating voltage exceeds this value the CHP efficiency of systems I and II decreases as a convex upward parabolic curve; however, depending on the fuel utilization ratio, the CHP efficiency of system I may linearly increase at a certain cell operating voltage.

Although the CHP efficiency of the systems obtained at the cell voltages of Group II is slightly smaller than that obtained at the cell voltages of Group I, the electrical efficiency of these systems obtained at the cell voltages of Group II is notably higher than that obtained at the cell voltages of Group I.

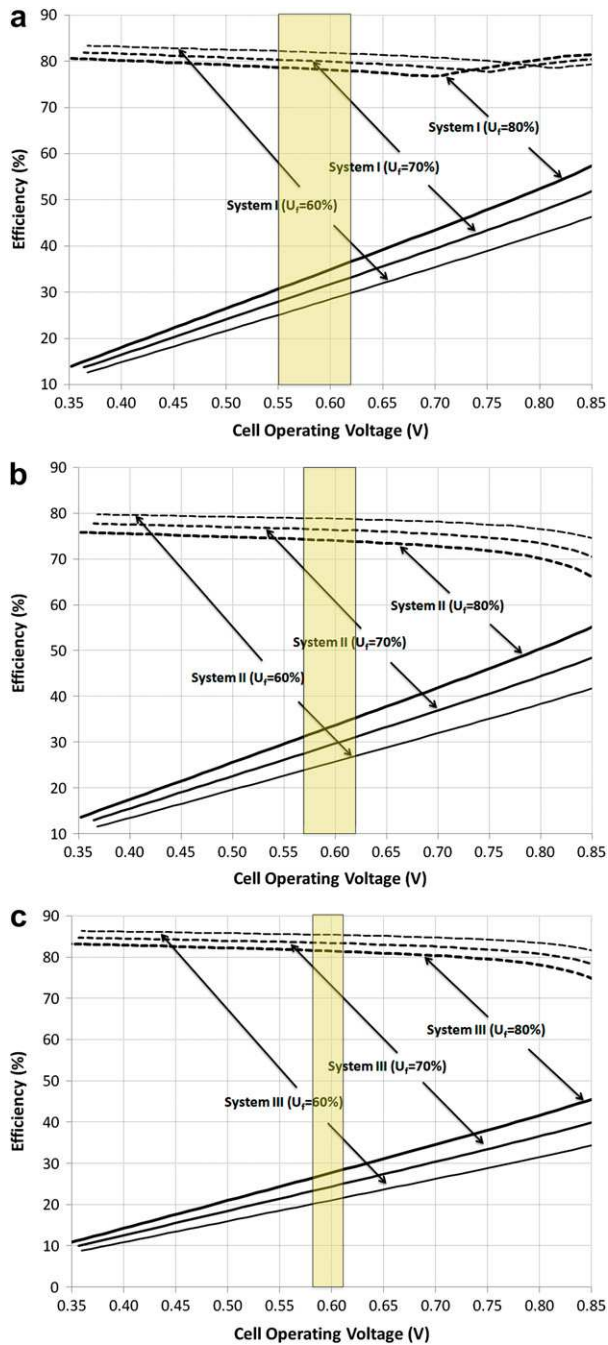


**Fig. 6** – Effect of the cell operating voltage at fuel utilization ratios of 80%, 70%, and 60%, on the net AC electrical efficiency (solid lines) and CHP efficiency (dashed lines) in (a) system I with anode exit gas recirculation, (b) system II with steam reforming, and (c) system III with partial oxidation fuel processor (the yellow column indicates the range of cell voltages at which the minimum number of cells is required in the SOFC stack operated with fuel utilization ratios between 60% and 80%).

### 6.2.3. Effect of the cell operating voltage and fuel utilization ratio on biogas fuel consumption

The effect of the cell operating voltage at fuel utilization ratios of 60%, 70%, and 80% on the biogas mass flow rate for all three systems studied are shown in Fig. 7. As shown in this figure,

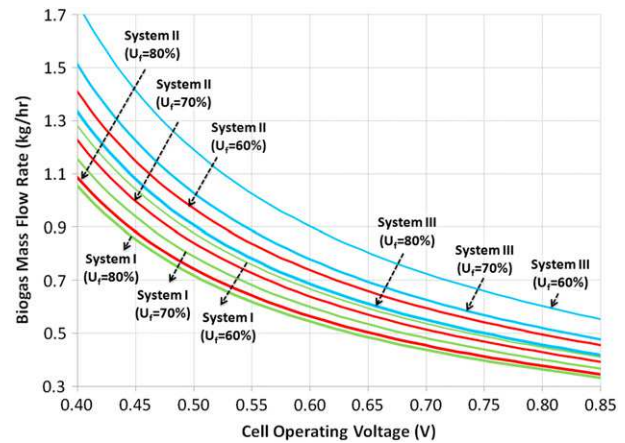


**Fig. 7** – Effect of the cell operating voltage at fuel utilization ratios of 80%, 70%, and 60%, on the inlet biogas mass flow rates in (a) system I with anode exit gas recirculation (green curves), (b) system II with steam reforming (red curves), and (c) system III with partial oxidation (blue curves) fuel processor.

with decreasing the cell voltage, the biogas mass flow rate increases progressively for all the systems studied. The higher the fuel utilization ratio, the lower the biogas mass flow rate required for the systems studied to generate 1 kW AC electric power. If the amount of the biogas fuel generated for a residential dwelling is limited to a certain value, this figure would be important to select an appropriate cell voltage and fuel utilization ratio for the systems studied.

### 6.2.4. Effect of the cell operating voltage and fuel utilization ratio on excess air

Fig. 8 shows the effect of the cell operating voltage at fuel utilization ratios of 60%, 70%, and 80% on the excess air required for controlling the temperature of the SOFC stack for

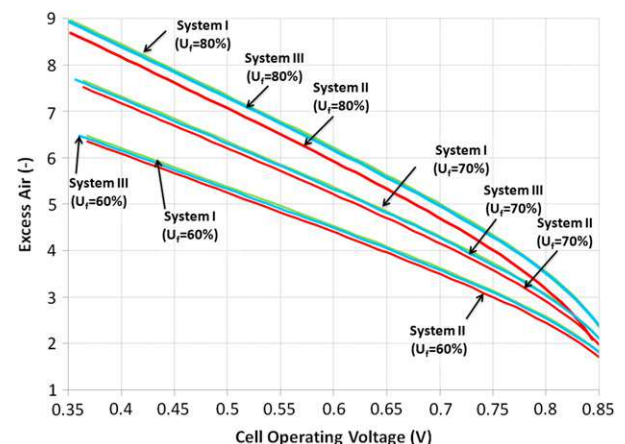


**Fig. 8** – Effect of the cell operating voltage at fuel utilization ratios of 80%, 70%, and 60%, on the excess air in (a) system I with anode exit gas recirculation (green curves), (b) system II with steam reforming (red curves), and (c) system III with partial oxidation (blue curves) fuel processor.

all three studied systems. As shown in this figure, the increase of the cell operating voltage leads to a decrease in the excess air; and so the size and initial investment cost for the air heater, blower, and burner decreases for all the systems studied. In the range of the fuel utilization ratio investigated, the excess air also decreases with decreasing the fuel utilization ratio.

Overall, the results of the sensitivity analysis indicate that with decreasing the cell operating voltage in Group I, the number of cells required for the SOFC stack increases, and the excess air required for controlling the SOFC stack temperature increases. Hence, the size and initial investment cost of the systems studied increase. The decrease in the cell operating voltage in this group also leads to a decrease in the electrical efficiency and an increase in the biogas consumption; however, the CHP efficiency does not change considerably. The TER of the systems studied also exceeds the TER required for the domestic hot water demands for single-family detached dwellings. Consequently, the optimum cell operating voltage is not in this group of the cell voltages and should be found in Group II. In fact, the lowest cell design voltage is limited to the cell voltage at which the minimum number of cells for the SOFC stack is obtained (mCV).

In Group II of the cell voltages, with increasing the cell operating voltage, the number of cells for the SOFC stack increases, whereas, the biogas consumption and excess air decrease. Therefore, a detailed economic analysis is required to find the cell design voltage in this group.

## 7. Conclusions

The results of this study indicate that biogas is a suitable fuel for residential applications of the SOFC systems studied. Due to the high carbon dioxide content of the biogas fuel, the amount of the reforming agent needed to prevent carbon deposition over the anode of ESC 4 cells decreases. For an SOFC stack with 27 ESC 4 cells operating at a fuel utilization ratio of 80%, the net AC electrical efficiency of 42.4%, 41.7%, and 33.9% is predicted for systems I to III, respectively. In these conditions, system III shows the highest CHP efficiency with 80.5%, followed by system I with 76.9%, and system II with 72.9%. The TER of systems I and II at the fuel utilization ratios of 70% and 80%, and system III at the fuel utilization ratio of 90%, is suitable to produce the electric power and hot water demands for single-family detached dwellings.

The exergy analysis shows that there is a considerable potential to generate additional electric power from the systems studied, especially from system III, if they are combined with other power generation devices and appropriately optimized.

The sensitivity analysis indicates that the optimum cell voltage is greater than the cell voltage at which the minimum number of cells for the SOFC stack is obtained. The minimum number of cells at the fuel utilization ratio of 80% is obtained at the cell voltage of 0.55 V for system I, 0.62 V for system II, and 0.61 V for system III. In these conditions, the number of ESC 4 cells required for the SOFC stack is 23 cells for systems I and II, and 24 cells for system III.

Overall, the biogas-fuelled SOFC systems studied show an appropriate performance to generate electric power and hot water demands for single-family detached dwellings.

## Acknowledgments

The authors gratefully acknowledge financial support provided by NSERC of Canada, EcoEnergy Technology Initiative Program, and AAFC-NRC Bioproducts Program.

## REFERENCES

- [1] Reddy AKN, Williams RH, Johansson TB. Energy after Rio: prospects and challenges. New York, NY: United Nations Development Program; 1997.
- [2] Athanasiou C, Coutelieres F, Vakouftsi E, Skoulou V, Antonakou E, Marnellos G, et al. From biomass to electricity through integrated gasification/SOFC system-optimization and energy balance. *Int J Hydrogen Energy* 2007;32:337–42.
- [3] Van herle J, Membrez Y, Bucheli O. Biogas as a fuel source for SOFC co-generators. *J Power Sources* 2004;127:300–12.
- [4] Shiratori Y, Oshima T, Sasaki K. Feasibility of direct-biogas SOFC. *Int J Hydrogen Energy* 2008;33:6316–21.
- [5] Farhad S, Yoo Y, Hamdullahpur F. Effects of fuel processing methods on industrial scale biogas-fuelled solid oxide fuel cell system for operating in wastewater treatment plants. *J Power Sources* 2010;195(5):1446–53.
- [6] Yentekakis IV, Papadam T, Goula G. Electricity production from wastewater treatment via a novel biogas-SOFC aided process. *Solid State Ionics* 2008;179:1521–5.
- [7] Van herle J, Maréchal F, Leuenberger S, Membrez Y, Bucheli O, Favrat D. Process flow model of solid oxide fuel cell system supplied with sewage biogas. *J Power Sources* 2004;131:127–41.
- [8] Jenne M, Dörk T, Schuler A. Proceedings of the Fifth European Solid Oxide Fuel Cell Forum. Lucerne, Switzerland; 2002:460–6.
- [9] Yi Y, Rao AD, Brouwer J, Samuelsen GS. Fuel flexibility study of an integrated 25kW SOFC reformer system. *J Power Sources* 2005;144:67–76.
- [10] Assabumrungrat S, Laosiripojana N, Pavarajarn V, Sangtongkitcharoen W, Tangitmatee A, Prasertthdam P. Thermodynamic analysis of carbon formation in solid oxide fuel cells with a direct internal reformer fueled by methanol. *J Power Sources* 2005;139:55–60.
- [11] Sangtongkitcharoen W, Assabumrungrat S, Pavarajarn V, Laosiripojana N, Prasertthdam P. Comparison of carbon formation boundary for different types of solid oxide fuel cells with methane feed. *J Power Sources* 2005;142:75–80.
- [12] Park EW, Moon H, Park M, Hyun SH. Fabrication and characterization of Cu–Ni–YSZ SOFC anodes for direct use of methane via Cu-electroplating. *Int J Hydrogen Energy* 2009;34:5537–45.
- [13] Hofmann Ph, Panopoulos KD, Fryda LE, Schweiger A, Ouweltjes JP, Karl J. Integrating biomass gasification with solid oxide fuel cells: effect of real product gas tars, fluctuations and particulates on Ni-GDC anode. *Int J Hydrogen Energy* 2008;33:2834–44.
- [14] Wang Y, Yoshida F, Kawase M, Watanabe T. Performance and effective kinetic models of methane steam reforming over Ni/YSZ anode of planar SOFC. *Int J Hydrogen Energy* 2009;34:3885–93.

- [15] Hofmann Ph, Panopoulos KD, Aravind PV, Siedlecki M, Schweiger A, Karl J, et al. Operation of solid oxide fuel cell on biomass product gas with tar levels  $>10 \text{ gNm}^{-3}$ . *Int J Hydrogen Energy* 2009;34(22):9203–12.
- [16] Achenbach E, Riensche E. Methane/steam reforming kinetics for solid oxide fuel cells. *J Power Sources* 1994;52:283–8.
- [17] Piroonlerkgula P, Laosiripojanab N, Adesinac AA, Assabumrungrat S. Performance of biogas-fed solid oxide fuel cell systems integrated with membrane module for  $\text{CO}_2$  removal. *Chem Eng Process* 2009;48:672–82.
- [18] Arteaga LE, Peralta LM, Kafarov V, Casas Y, Gonzales E. Bioethanol steam reforming for ecological syngas and electricity production using a fuel cell SOFC system. *Chem Eng J* 2008;136:256–66.
- [19] Peksen M, Peters R, Blum L, Stolten D. Numerical modelling and experimental validation of a planar type pre-reformer in SOFC technology. *Int J Hydrogen Energy* 2009;34:6425–36.
- [20] Chan SH, Ding OL. Simulation of a solid oxide fuel cell power system fed by methane. *Int J Hydrogen Energy* 2005;30:167–79.
- [21] Piroonlerkgul P, Assabumrungrat S, Laosiripojana N, Adesina AA. Selection of appropriate fuel processor for biogas-fuelled SOFC system. *Chem Eng J* 2008;140:341–51.
- [22] Hotz N, Senn SM, Poulidakos D. Exergy analysis of a solid oxide fuel cell micropowerplant. *J Power Sources* 2006;158:333–47.
- [23] Franzoni A, Magistri L, Traverso A, Massardo AF. Thermoeconomic analysis of pressurized hybrid SOFC systems with  $\text{CO}_2$  separation. *Energy* 2008;33:311–20.
- [24] Modafferi V, Panzera G, Baglio V, Frusteri F, Antonucci PL. Propane reforming on Ni–Ru/GDC catalyst:  $\text{H}_2$  production for IT-SOFCs under SR and ATR conditions. *Appl Catal A Gen* 2008;334:1–9.
- [25] Akkaya AV, Sahin B, Erdem HH. An analysis of SOFC/GT CHP system based on exergetic performance criteria. *Int J Hydrogen Energy* 2008;33:2566–77.
- [26] Peters R, Riensche E, Cremer P. Pre-reforming of natural gas in solid oxide fuel-cell systems. *J Power Sources* 2000;86:432–41.
- [27] Kazempoor P, Dorer V, Ommi F. Evaluation of hydrogen and methane-fuelled solid oxide fuel cell systems for residential applications: system design alternative and parameter study. *Int J Hydrogen Energy* 2009;34:8630–44.
- [28] Sammes NM, Boersma R. Small-scale fuel cells for residential applications. *J Power Sources* 2000;86:98–110.
- [29] Lee KH, Strand RK. SOFC cogeneration system for building applications, part 1: development of SOFC system-level model and the parametric study. *Renewable Energy* 2009;34:2831–8.
- [30] Barrera R, De Biase S, Ginocchio S, Bedogni S, Montelatici L. Performance and life time test on a 5kW SOFC system for distributed cogeneration. *Int J Hydrogen Energy* 2008;33:3193–6.
- [31] Bompard E, Napoli R, Wan B, Orsello G. Economics evaluation of a 5kW SOFC power system for residential use. *Int J Hydrogen Energy* 2008;33:3243–7.
- [32] Alanne K, Saari A, Ugursal VI, Goodc J. The financial viability of an SOFC cogeneration system in single-family dwellings. *J Power Sources* 2006;158:403–16.
- [33] Braun RJ, Kleina SA, Reindla DT. Evaluation of system configurations for solid oxide fuel cell-based micro-combined heat and power generators in residential applications. *J Power Sources* 2006;158(2):1290–305.
- [34] Braun RJ, Klein SA, Reindl DT. Considerations in the design and application of solid oxide fuel cell energy systems in residential markets. *ASHRAE Trans* 2004;110(1):14–24.
- [35] Wheeldon I, Caners C, Karan K, Peppley B. Utilization of biogas generated from ontario wastewater treatment plants in solid oxide fuel cell systems: a process modeling study. *Int J Green Energy* 2007;4:221–31.
- [36] Farhad S, Hamdullahpur F. Developing fuel map to predict the effect of fuel composition on the maximum voltage of solid oxide fuel cells. *J Power Sources* 2009;191(2):407–16.
- [37] Farhad S, Hamdullahpur F. Developing fuel map to predict the effect of fuel composition on the maximum efficiency of solid oxide fuel cells. *J Power Sources* 2009;193(2):632–8.
- [38] Yan R, Liang DT, Tsen L, Tay JH. Kinetics and mechanism of  $\text{H}_2\text{S}$  adsorption by alkaline activated carbon. *Environ Sci Technol* 2002;36:4460–6.
- [39] Chan SH, Khor KA, Xia ZT. A complete polarization model of a solid oxide fuel cell and its sensitivity to the change of cell component thickness. *J Power Sources* 2001;93:130–40.
- [40] Virkar AV, Chen J, Tanner CW, Kim J. The role of electrode microstructure on activation and concentration polarizations in solid oxide fuel cells. *Solid State Ionics* 2000;131:189–98.
- [41] Kim JW, Virkar AV, Fung KZ, Mehta K, Singhal SC. Low temperature, high performance anode-supported solid oxide fuel cells. *J Electrochem Soc* 1999;146(1):69–78.
- [42] Colpan CO, Hamdullahpur F, Dincer I, Yoo Y. Effect of gasification agent on the performance of solid oxide fuel cell and biomass gasification systems. *Int J Hydrogen Energy*; 2009;. doi:10.1016/j.ijhydene.2009.08.083.
- [43] Younessi-Sinaki M, Matida EA, Hamdullahpur F. Kinetic model of homogeneous thermal decomposition of methane and ethane. *Int J Hydrogen Energy* 2009;34(9):3710–6.
- [44] H.C. Starck Company, [www.hcstarck-ceramics.com/](http://www.hcstarck-ceramics.com/) (accessed April 2009).
- [45] Hofmann Ph, Schweiger A, Fryda L, Panopoulos KD, Hohenwarter U, Bentzen JD, et al. High temperature electrolyte supported Ni-GDC/YSZ/LSM SOFC operation on two-stage Viking gasifier product gas. *J Power Sources* 2007;173:357–66.
- [46] Szargut J, Morris DR, Steward FR. Exergy analysis of thermal, chemical, and metallurgical processes. Hemisphere Publishing Corporation; 1988.
- [47] Farhad S, Saffar-Avval M, Younessi-Sinaki M. Efficient design of feedwater heaters network in steam power plants using pinch technology and exergy analysis. *Int J Energy Research* 2007;32(1):1–11.
- [48] Farhad S, Younessi-Sinaki M, Golriz MR, Hamdullahpur F. Exergy analysis and performance evaluation of CNG to LNG converting process. *Int J Exergy* 2008;5(2):164–76.
- [49] Nietsch T, Clark J. Market Oriented Design Studies for SOFC Based Systems. ETSU Report F/0.1/00129/REP; 1999.
- [50] Farhad S, Hamdullahpur F. Conceptual design of a novel ammonia-fuelled portable solid oxide fuel cell system. *J Power Sources* 2010;195:3084–90.